Kink Propagation in a Highly Discrete System: Observation of Phase Locking to Linear Waves

Herre S. J. van der Zant* and Terry P. Orlando
Department of Electrical Engineering and Computer Science, Massachusetts Institute of Technology, Cambridge, Massachusetts 02139

Shinya Watanabe and Steven H. Strogatz†
Department of Mathematics, Massachusetts Institute of Technology, Cambridge, Massachusetts 02139
(Received 25 May 1994)

We report the first observation of phase locking between a kink propagating in a highly discrete system and the linear waves excited in its wake. The current-voltage (I-V) characteristics of discrete rings of Josephson junctions have been measured. Resonant steps appear in the I-V curve, due to phase locking between a propagating vortex and its induced radiation. Unexpectedly, mode numbers outside the first Brillouin zone are physically relevant, due to the nonlinearity of the system.

PACS numbers: 74.50.+r, 05.45.+b, 74.40.+k

The discrete sine-Gordon equation governs the dynamics of many physical systems, such as dislocations, chains of coupled pendula, magnetic and ferroelectric domain walls, and arrays of Josephson junctions. Unlike the continuous sine-Gordon equation [1], very little is known about the dynamics of the discrete sine-Gordon equation. It appears that an essential feature introduced by discreteness is the generation of radiation by a moving kink. Early simulations by Currie *et al.* [2] showed that when a kink propagates in a highly discrete one-dimensional (1D) lattice, it excites small-amplitude linear waves in its wake. This effect was explained analytically by Peyrard and Kruskal [3], who also found that in the absence of external driving, kinks propagate preferentially at a particular set of velocities. Recently, in simulations of a discrete ring of underdamped Josephson junctions, Ustinov *et al.* [4] found that vortices circulating around the ring can become phase locked with their induced radiation; the predicted signature of this effect is a series of novel resonance steps in the current-voltage (I-V) curve.

In this Letter, we report the first observation of phase locking between a vortex circulating in a discrete Josephson ring and the radiation excited in its wake. To the best of our knowledge, our measurements also provide the first (indirect) experimental evidence for the predicted generation of linear waves by a kink propagating in a highly discrete system [2,3]. Our experimental findings are in quantitative agreement with the predictions of a discrete sine-Gordon model [4]. This close agreement suggests that the Josephson rings studied here are promising systems for future investigations of nonlinear wave propagation in discrete lattices.

Figure 1 shows a schematic drawing of our discrete Josephson ring. The system is governed by the discrete sine-Gordon equation,

$$\frac{\ddot{\phi}_i}{\omega_p^2} + \frac{\Gamma}{\omega_p}\dot{\phi}_i + \sin\phi_i = \Lambda_J^2\nabla^2\phi_i + \frac{I_i}{I_c}, \qquad (1)$$

for $i = 1, \ldots, N$. Here ϕ_i is the phase difference across the ith junction, N is the number of junctions, $\nabla^2\phi_i = \phi_{i+1} - 2\phi_i + \phi_{i-1}$ is the discrete Laplacian, and the overdots denote differentiation with respect to time. The discreteness parameter Λ_J^2 is defined as $\Lambda_J^2 = L_J/L_s$, where $L_J = \Phi_0/2\pi I_c$ is the Josephson inductance, Φ_0 is the flux quantum, I_c is the junction critical current, and L_s is the self-inductance of a single cell. Measured in cell spacings, the penetration depth for the current and field distributions is Λ_J. The junction plasma frequency $\omega_p = 1/\sqrt{L_J C}$, where C is the junction capacitance. The damping parameter Γ is the reciprocal of the square root of the Stewart-McCumber parameter β_c. The last term is the applied current at node i, normalized to I_c. The boundary condition is $\phi_{i+N} = \phi_i + 2\pi M$, where M is the number of vortices (fluxons) trapped in the ring.

The rings used in our experiments consist of $N = 8$ high-quality Nb-Al_2-O_x-Nb junctions and are fabricated with a four mask selective-niobium-anodization process at AT&T Bell Laboratories and MIT Lincoln Labora-

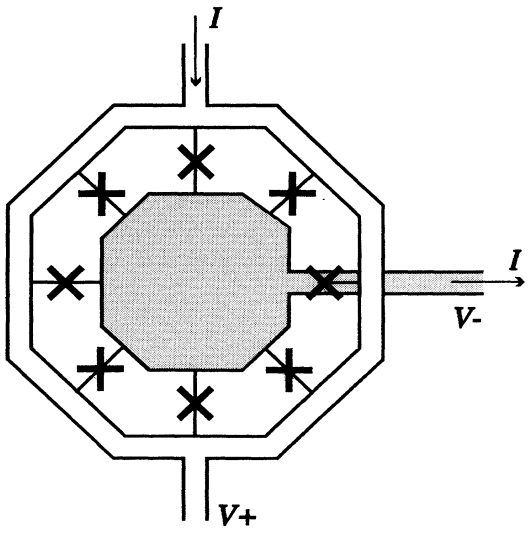

FIG. 1. Schematic drawing of a discrete ring of 8 Josephson junctions.

 0031-9007/95/74(1)/174(4)$06.00

tory. The outer diameter of the ring is 48 μm and the Josephson junctions have areas of 2 μm^2. The junction capacitance $C = 95$ fF [5], so that charging effects are negligible. The normal-state array resistance $R_{n,\text{array}}$ is measured just below the niobium critical temperature T_c. The junction normal-state resistance is then assumed to be $R_n = NR_{n,\text{array}}$. The junction critical current $I_c(T)$ follows the Ambegaokar-Baratoff temperature dependence with $I_c(0)R_n = 1.9$ mV. For the temperatures of interest, our junctions are underdamped, i.e., $\beta_c(R_n) = 2\pi I_c R_n^2 C/\Phi_0 \gg 1$. As illustrated in Fig. 1, the transport current is applied to a single node of the array and extracted from the inner island, while at the same time the voltage can be measured across the outer and inner niobium islands. Arrays are measured in a ^{4}He probe with standard equipment. At room temperature the leads are filtered with radio-frequency-interference filters with a cutoff frequency of 10 kHz. Inside the vacuum can, a small magnet produces a magnetic field perpendicular to the array.

Figure 2 plots typical I-V curves for rings cooled down in different applied magnetic fields. Cooling down in a field of about M flux quanta Φ_0 corresponds to trapping exactly M vortices in the ring. When the ring is cooled through T_c in zero field, the I-V curve shows a depinning current and jumps to the gap voltage at $0.84NI_c$. With $M = 1$ applied to the ring, the depinning current vanishes and a current step appears near $V = 0.2$ mV. The jump to the gap voltage now occurs at $I_{\max} = 0.55NI_c$. For $M = 2$, 3, and 4, the voltage position of the steps increases to about 0.35, 0.43, and 0.48 mV, respectively. On the other hand, the I-V curves for $5\Phi_0$, $6\Phi_0$, $7\Phi_0$, and $8\Phi_0$ are identical to those when cooling down with $3\Phi_0$, $2\Phi_0$, $1\Phi_0$, and $0\Phi_0$. Thus, a total of four different peaks can be observed in our ring of 8 junctions. This result has been reproduced in experiments on several other rings.

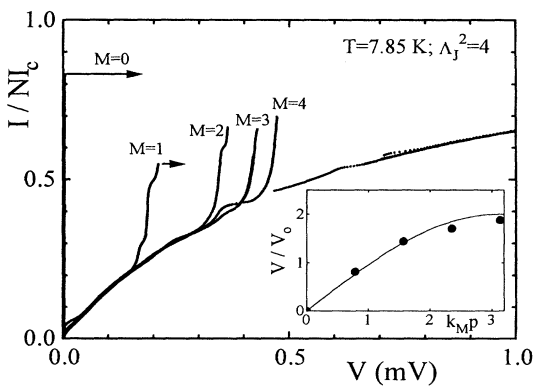

FIG. 2. Experimental I-V curves corresponding to the five possible situations with M vortices trapped in a Josephson ring of 8 junctions. Measured parameters: $\Lambda_J^2 = 4.0$, $\beta_c(R_n) = 33$. Inset: voltage position of the steps (normalized to V_0) vs wave number $k_M p$. Curve is a fit by Eq. (2) with $V_0 = 0.25$ mV.

The absence of a depinning current for $M = 1$ (Fig. 2) agrees with calculations [6] which show that the energy barrier for propagation of a single vortex is negligible if $\Lambda_J^2 > 1$. The $M = 4$ curve exhibits a small depinning current, indicating that interactions among the four trapped vortices start to play a role. Figure 2 also shows that $I_{\max}$ increases with M. This increase has been predicted by Marcus and Imry [7]. Their analysis indicates that the jump to the gap voltage occurs when the current reaches the I-V curve of a single resistively shunted Josephson junction with critical current NI_c. In particular, this predicts that for continuous rings $I_{\max}$ should always exceed NI_c. Their preliminary results on discrete arrays [7], however, show upper-current thresholds significantly lower than NI_c. This is consistent with our experimental data, as well as with our simulations of Eq. (1). We find numerically that $I_{\max}$ decreases when the system becomes more underdamped and that $I_{\max}$ in the simulations differs by less than 15% from the measured value.

In contrast to the experiments on continuous Josephson rings [8,9], the voltages of the steps shown in Fig. 2 are not proportional to M. We have performed [5] a linear analysis ($\Lambda_J^2 \gg 1$) of 1D parallel arrays with free boundaries. In such a system, resonances occur at voltages determined by the dispersion relation $\omega(k)$ of a 1D discrete, linear transmission line of inductances L_s and capacitances C. A similar analysis for a ring geometry with lattice spacing of p yields that the resonant voltage peaks V_M are given by

$$V_M/V_0 = 2|\sin(k_M p/2)|, \tag{2}$$

where the wave number $k_M = 2\pi M/Np$, with $M = -N/2, \ldots, -1, 0, 1, \ldots, N/2$, and where $V_0 = \Phi_0/2\pi\sqrt{L_s C}$. This equation indicates that, in an $N = 8$ system, one only expects to see four different resonant peaks in accordance with our experimental observation.

In the inset of Fig. 2, we plot the voltage position of the resonances as a function of $k_M p$. The solid line is Eq. (2) with fitting parameter $V_0 = 0.25$ mV indicating that $L_s = 18.5$ pH, a reasonable value for our geometry. The two data points near the Brillouin zone edge ($k_M p = \pi$) are somewhat lower than predicted by Eq. (2), due to mutual-inductance interactions between cells in the ring [5].

In the experiment, we find that the I-V curves are smooth only for high Λ_J^2 values; when Λ_J^2 is decreased by lowering the temperature, fine structure becomes visible. At the same time the maximum voltage predicted by Eq. (2) is not reached. These observations are consequences of the nonlinear dynamics in discrete arrays. Figure 3 shows the fine structure in the current-voltage characteristic of a single vortex ($M = 1$) trapped in the ring for $\Lambda_J^2 = 2.2$. In total, six resonant steps are present, corresponding to local minima in the differential resistance dV/dI.

To clarify the physical origin of the resonances, it is helpful to recall a mechanical analog of the system. The discrete sine-Gordon equation (1) may be viewed

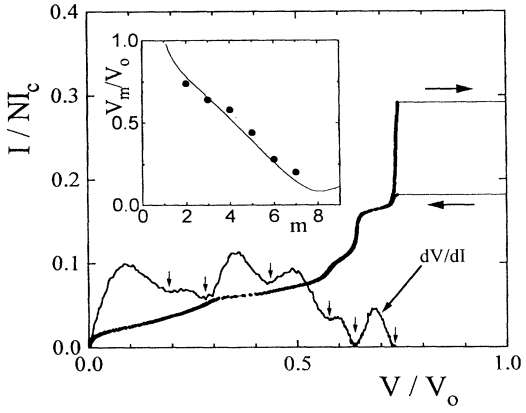

FIG. 3. Experimental I-V curve for one vortex trapped in the ring measured at 6.4 K, where $\Lambda_J^2 = 2.2$ and $\beta_c(R_n) = 61$. The solid line shows dV/dI; note six dips corresponding to six resonant steps in the I-V curve. Inset: voltage position of these six steps vs mode number m. Curve is a fit by Eq. (3) with $\Lambda_J^2 = 2.2$.

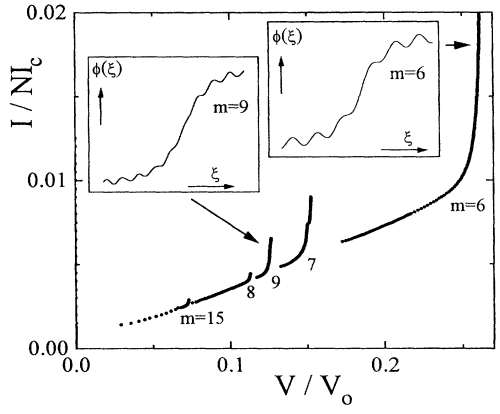

FIG. 4. Numerical I-V curve for Eq. (1) with $M = 1$, $N = 8$, $\Gamma = 0.02$, and $\Lambda_J^2 = 1$. The mode number m of linear waves is indicated below each step. Inset: traveling waves with $m = 6$ and $m = 9$.

as the equation of motion for a ring of N pendula, each of which is viscously damped, driven by a constant torque, and coupled to its nearest neighbors by torsional springs. A vortex corresponds to a kink traveling around the ring. In this configuration, a given pendulum hangs almost straight down for much of the time, but when the kink passes by, the pendulum overturns rapidly. Then, because the pendulum is underdamped, it "rings" for several oscillations. This ringing is the analog of the radiation excited by the kink. A resonance occurs if the pendulum rings precisely an integer number of times between successive passages of the kink.

The voltages of the resonant steps can be predicted from these considerations. The possible ringing frequencies are the lattice eigenfrequencies of small oscillations about the kink, and the circulation frequency of the kink is proportional to the voltage position of the step. By matching the circulation period to an integer multiple m of ringing periods, the following formula is obtained for the resonant voltages:

$$\frac{V_m}{V_0} = \frac{1}{m}[\Lambda_J^{-2} + 4\sin^2(\pi m/N)]^{1/2}. \quad (3)$$

In the inset of Fig. 3, the drawn line is Eq. (3) with $V_0 = 0.25$ mV. There is good agreement between the model and our experiment.

A formula equivalent to Eq. (3) was first obtained in Ref. [4], by matching the kink velocity to the phase velocity of the radiated waves. This condition is appropriate because numerical simulations indicate that the radiation is stationary in the frame of the moving kink; the linear waves are phase locked to the kink, and together they form a traveling wave. Two examples of such traveling waves are given in the insets of Fig. 4, where $\phi_j(t) = \phi(\xi)$ is the traveling wave, $\xi = jp - ut$ is the coordinate in the kink frame, and u is the kink velocity. The integer m can now be visualized as the number of small oscillations superimposed on the kink wave form, i.e., m is the mode number of the linear waves.

Equation (3) has peculiar consequences. Ordinarily, one expects that in a discrete ring of N junctions, only $N/2$ steps are distinct, or perhaps N at most, as assumed in [4]. But because Eq. (3) is not periodic in the mode number m, the voltages V_m and V_{m+N} are predicted to be different for all m. Thus it seems that m can take values outside the first Brillouin zone, up to $m = \infty$, at least in principle. To test this idea, we integrated Eq. (1) numerically and generated I-V curves. As in the experiments, I was slowly swept up and down several times, and for each I, the solution was allowed to converge to an attractor. The existence of steps with $m > N$ is confirmed by the I-V curve shown in Fig. 4 [10]. The mode numbers m, given at the base of the steps, were determined by carefully examining the wave forms $\phi_j(t)$. As shown in Fig. 4 (inset), a wave form with $m = 9$ small oscillations can occur in a ring of $N = 8$ junctions. The corresponding step lies between the $m = 7$ and $m = 8$ steps; this is expected from Eq. (3), which predicts that V_m is nonmonotonic in m, and specifically that V_9 lies between V_7 and V_8. The nonmonotonicity also explains why the steps for $m = 10, \ldots, 14$ are not visible in Fig. 4; they are hidden under the stronger resonances for $m = 7, \ldots, 9$, which occur at approximately the same positions. The location of the next detectable step, corresponding to $m = 15$, is well predicted by Eq. (3).

The physical relevance of mode numbers outside the first Brillouin zone is readily understood in terms of the pendulum analog. The integer m is the number of times each pendulum oscillates between consecutive sweeps of the circulating kink. This number can be arbitrarily large, if the kink is moving sufficiently slowly

(as it will be, near the bottom of the I-V curve). Of course, in a *linear* discrete system, one cannot distinguish between mode m and $m + N$; the difference is that there is nothing analogous to a circulating kink in a linear system. The rotation of the kink—an inherently *nonlinear* phenomenon—provides the crucial reference that allows one to discriminate mode m from $m + N$.

Our results suggest that 1D discrete Josephson rings are not only promising model systems for the study of nonlinear lattices, but also for future experiments on ballistic and quantum vortices. On a resonant step, a moving vortex couples to linear waves; further increases of the current do not lead to further increases in the vortex velocity, because the energy is consumed in amplifying the linear waves. In this sense, the coupling to linear waves can be viewed as an additional source of damping for the vortex. Away from the resonant steps, the loss mechanism is Ohmic dissipation in the junctions crossed by the moving vortex. In underdamped tunnel junctions this dissipation can be very small, indicating nearly free propagation of vortices, especially if $\Lambda_J > 1$, where there is also a negligible barrier for vortex motion. For example, we have estimated the mean free path [11] in our samples to be about 15 circumferences at 4.2 K, and much larger in arrays with lower damping at lower temperatures. Therefore, underdamped arrays with $\Lambda_J > 1$ at low temperatures are in the appropriate regime for studies of ballistic vortex motion [11], quantum interference of vortices [12,13], and persistent motion of vortices around a charge [14,15].

We thank Kevin Delin, Mark Ketchen, Alan Kleinsasser, and Ron Miller for valuable discussions. This research supported in part by NSF Grants No. DMR-9402020, No. DMS-9057433, and No. DMS-9111497. We also acknowledge the support of AT&T, IBM, and MIT Lincoln Laboratory in the fabrication of the samples.

*Present address: Kamerlingh Onnes Laboratory, Leiden University, P.O. Box 9506, 2300 RA Leiden, The Netherlands.

†Present address: Theoretical and Applied Mechanics, Cornell University, Ithaca, NY 14853.

[1] Yu. S. Kivshar and B. A. Malomed, Rev. Mod. Phys. **61**, 763 (1989).

[2] J. F. Currie, S. E. Trullinger, A. R. Bishop, and J. A. Krumhansl, Phys. Rev. B **15**, 5567 (1977).

[3] M. Peyrard and M. D. Kruskal, Physica (Amsterdam) **14D**, 88 (1984).

[4] A. V. Ustinov, M. Cirillo, and B. A. Malomed, Phys. Rev. B **47**, 8357 (1993).

[5] H. S. J. van der Zant, D. Berman, K. A. Delin, and T. P. Orlando, Phys. Rev. B **49**, 12 945 (1994).

[6] R. D. Bock, J. R. Phillips, H. S. J. van der Zant, and T. P. Orlando, Phys. Rev. B **49**, 10 009 (1994).

[7] P. M. Marcus and Y. Imry, Solid State Commun. **33**, 345 (1980).

[8] A. Davidson, B. Dueholm, and N. F. Pedersen, J. Appl. Phys. **60**, 1447 (1986).

[9] A. V. Ustinov, T. Doderer, R. P. Huebener, N. F. Pedersen, B. Mayer, and V. A. Oboznov, Phys. Rev. Lett. **69**, 1815 (1992).

[10] In our experiment, the high wave-number resonances are smoothed out because Λ_J^2 and Γ are too large. Simulations indicate that the steps can be observed for $\Lambda_J \leq 1$ and $\Gamma \leq 0.05$.

[11] H. S. J. van der Zant, F. C. Fritschy, T. P. Orlando, and J. E. Mooij, Phys. Rev. Lett. **66**, 2531 (1991); Europhys. Lett. **18**, 343 (1992).

[12] W. J. Elion, J. J. Wachters, L. L. Sohn, and J. E. Mooij, Phys. Rev. Lett. **71**, 2311 (1993).

[13] B. J. van Wees, Phys. Rev. Lett. **65**, 255 (1990).

[14] T. P. Orlando and K. A. Delin, Phys. Rev. B **43**, 8717 (1991).

[15] Z. Hermon, A. Stern, and E. Ben-Jacob, Phys. Rev. B **49**, 9757 (1994).